Pergamon

Int. J. Heat Mass Transfer. Vol. 37, Suppl. 1, pp. 113–122, 1994

0017-9310/94 $6.00 + 0.00

0017-9310(93)E0053-J

Determination of the characteristic and diffusion times of polyacrylamide solutions using falling balls and needles

SANG-SIN YOO, CHAN-YEAL JEON† and Y. I. CHO‡

Department of Mechanical Engineering and Design, Hankuk Aviation University, Koyangshi, Kyonggido, Korea

Abstract—The present study determined the apparent viscosity and the characteristic time of aqueous polyacrylamide Separan AP-273 solutions by using a falling ball viscometer. Two laser beams and a digital timer system were used to accurately measure the terminal velocity of a falling ball or needle in the falling ball viscometer. The diffusion time of the polyacrylamide solution was determined by measuring the terminal velocities of falling balls. A consistent diffusion time was observed for balls, whereas in the case of needles, the diffusion time depended on the ratio of the needles' length to their diameters. The diffusion time decreased as the ratio increased for a given Separan solution. The characteristic time and the diffusion time of the polyacrylamide solution decreased as degradation continued. The effect of degradation on the heat transfer was more significant than that on the friction factor. A computer-aided image-processing technique was employed to visualize the flow phenomena around balls. For a time interval of 3 min, recirculating eddies were formed both upstream and downstream of the falling ball, whereas for a time interval of 10 min the eddies disappeared.

INTRODUCTION

A NUMBER of studies have used a falling ball viscometer to determine the viscosity of a highly viscous fluid by measuring the terminal velocity of a falling ball. The terminal velocity may be measured accurately in a vertical test cylinder containing the highly viscous fluid. However, the measurement of the terminal velocity in a less viscous fluid is a difficult task if one uses a traditional timer system with a stopwatch, because the time taken for a ball to travel a given distance in the test cylinder is too short to measure accurately.

Turian [1] and Gottlieb [2] determined the viscosity of non-Newtonian fluids using stainless steel balls in a falling ball viscometer by adopting Tanner's wall correction equation which was originally developed for Newtonian fluids. Cho [3] measured the viscosity of aqueous polyacrylamide Separan AP-273 solutions with concentrations from 5000 to 10000 w.p.p.m. using a falling ball viscometer. Cho was able to measure the viscosity at a low rate of shear ($0.1\ s^{-1}$) by using aluminum, Teflon, and nylon balls, which are much lighter than stainless steel balls. Cho *et al.* [4] reported some difficulty in measuring the terminal velocity for a 2000 w.p.p.m. polyacrylamide solution in the falling ball viscometer because of the above-mentioned reason and applied a Weissenberg Rheogoniometer to measure the viscosity of the polyacrylamide solution.

Cho *et al.* [4] determined the characteristic time of the polyacrylamide solutions of 2000–10000 w.p.p.m.: the zero-shear-rate viscosity was obtained using the Weissenberg Rheogoniometer. The viscosity in the intermediate range of shear rate was obtained using the falling ball viscometer, and the infinite-shear-rate viscosity was obtained using a capillary tube, respectively. Kanchanalakshana and Ghajar [5] used hollow balls partly filled with water to measure the viscosity of low concentration polyacrylamide solutions (500–1000 w.p.p.m.) at low shear rates. However, they could not determine the zero-shear-rate viscosity of the polyacrylamide solutions with the falling ball viscometer, even with hollow balls. To compensate for this limitation, Park [6] employed a falling needle viscometer in which needles were dropped in a vertical cylinder. Since the densities of the needles could be varied at values slightly larger than test fluid densities, Park and Irvine [7] were able to measure the viscosity of a 2000 w.p.p.m. polyacrylamide solution to a very low rate of shear ($10^{-4}\ s^{-1}$).

Cho [3] reported the presence of the diffusion time of an aqueous viscoelastic solution, defined as the time at which the terminal velocity of a falling ball was not affected by the time interval of dropping balls. The diffusion time was consistently observed when a ball was used in the falling ball viscometer. Park and Irvine [7] observed the diffusion time when a ball was used but did not observe the time when needles were used. Since the geometry of the needles used by Park and Irvine was limited to a certain range, we may speculate that the diffusion time might depend on the length

† Present address: Department of CAD/CAM, Inchon Industrial College, Gusandong, Bukku, Inchon, Korea.

‡ Present address: Department of Mechanical Engineering and Mechanics, Drexel University, Philadelphia, PA 19104, U.S.A.

NOMENCLATURE

C_d	drag coefficient	η_a	apparent viscosity
d	ball or needle diameter	$\bar{\eta}$	normalized viscosity
f	Fanning friction factor, $\tau_w/(\rho V^2/2)$	λ_1	characteristic time [s]
L	needle length	λ_2	diffusion time [s]
n	power-law exponent	τ	shear stress.
Nu	Nusselt number		
Pr	Prandtl number		
Re	Reynolds number		
V	average or terminal velocity	Subscripts	
w.p.p.m.	weight parts per million.	a	property based on apparent viscosity
Greek symbols		0	zero-shear-rate
$\dot{\gamma}$	shear rate [s^{-1}]	∞	infinite-shear rate.

of a needle or the ratio of the needle's length to its diameter.

Based on the flow visualization results around a cylinder, James and Acosta [8] reported differences in flow fields for water and a 30 w.p.p.m., aqueous Polyox solution. Flow visualization experiments by Metzner [9] showed markedly different flow patterns between Newtonian and non-Newtonian fluids when two fluids entered a small tube from a large reservoir. Metzner and White [10] and Metzner *et al.* [11] reported that, when the flow field was suddenly accelerated, as it is in the inlet of the small tube, the streamlines of a non-Newtonian fluid were quite different from those of a Newtonian fluid. Recently, a computer-aided image-processing technique has been widely used for flow field visualizations, refs. [12–14], so that streamline images could significantly be enhanced by virtue of a digital filtering technique.

The objective of the present study is to determine the apparent viscosity of relatively dilute polyacrylamide solutions (both those that are fresh and those that are undergoing mechanical degradation) over a wide range of shear rates in order to determine the characteristic time and diffusion time of the solutions. In order to understand the origin of the diffusion time of the polyacrylamide solution observed with balls, the present study uses an image-processing technique to visualize the flow around a falling ball under different conditions. Degradation effects of the dilute polyacrylamide solutions on flow and heat transfer behavior are analysed in terms of the variation of the characteristic time and the diffusion time.

EXPERIMENTAL

The falling ball viscometer used in the present study consisted of two helium–neon gas lasers (output = 5 mW; beam diameter = 0.9 mm), a digital timer system, a test cylinder, a constant temperature circulator, and adapters. Adapters were designed to guide the falling matters such as stainless steel balls, aluminum balls and needles to the exact center of the test cylinder. A schematic diagram of the experimental set-up is shown in Fig. 1. Two lasers were installed at 400 and 500 mm away from the top of the circular cylinder, respectively. The lasers were aligned to ensure both laser beams passed through the center of the cylinder. When a ball or a needle travels along the center of the cylinder and cuts off the laser beams, the time taken for the ball or the needle to travel the given distance (i.e. 100 mm) was recorded in the digital timer system. The time system was designed to measure time intervals from 0.001 s to 60 min.

In the present study stainless steel balls, whose diameters and densities are given in Table 1, were used to provide viscosity data at relatively high shear rates. Since the densities of the stainless steel balls were far greater than that of an aqueous polymer solution, hollow aluminum balls were used for viscosity data in the low and intermediate shear rate range.

In order to adjust the densities of hollow balls, a

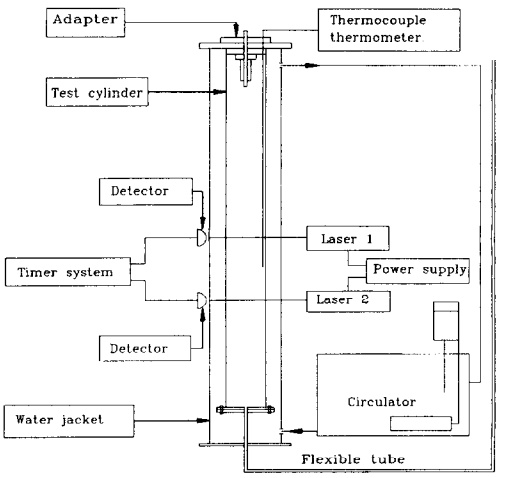

FIG. 1. Schematic diagram of a falling ball viscometer.

Table 1. Diameter and density of stainless steel balls

Ball No.	Diameter $\times 10^{-3}$ m	Mass $\times 10^{-3}$ kg	Density (kg m^{-3})
1	1.9966	0.0419	7673.7
2	2.9967	0.1093	7759.1
3	3.9986	0.2600	7768.1
4	4.9943	0.5072	7777.1
5	6.9960	0.8779	7772.1

Table 2. Diameter and density of hollow aluminum balls

Ball No.	Diameter $\times 10^{-3}$ m	Mass $\times 10^{-3}$ kg	Density (kg m^{-3})
1	9.50	0.4474	996.6
2	9.50	0.4509	1004.1
3	9.52	0.4575	1012.7
4	9.50	0.5159	1149.2
5	9.50	0.8095	1803.4
6	9.52	1.1012	2437.6

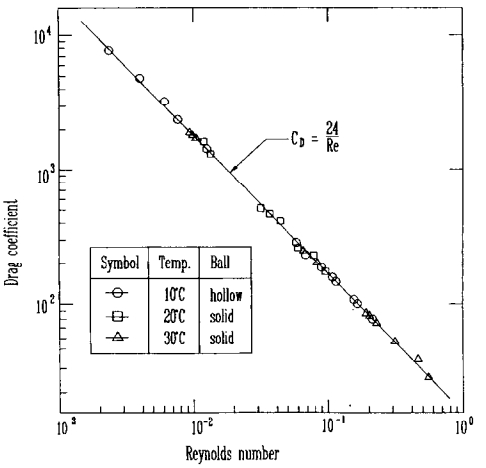

FIG. 2. Drag coefficient of a sphere vs the Reynolds number for 92% glycerin solution.

small hole of 0.3 mm was drilled on the surface of each hollow ball, and iron powder was inserted into the ball. The hole was closed with silicone rubber adhesive sealant, and the surface was finished using a fine sandpaper. This procedure made it possible to adjust the density of the hollow ball until it was very close to the density of aqueous test solutions. Table 2 shows the diameter and density of hollow aluminum balls.

Needles were made of cylindrical glass tubes. Iron powder was also inserted into the tube to adjust the densities of the needles. Two ends of the glass tube were rounded to secure semi-spherical shapes. The dimension and density of the needles used in the present study are given in Table 3.

The capillary tube viscometer consisted of a reservoir, a constant temperature circulator, a pressure tank and a capillary tube. The capillary tube viscometer was used to measure the viscosity at high shear rates, including the infinite-shear-rate viscosity. A detailed description of the capillary tube viscometer has been given elsewhere [15, 16].

An aqueous 92% glycerin solution (Duksan Chemical Co., Korea) was used as a Newtonian fluid in order to verify the accuracy of the present experimental apparatus and procedure. Aqueous polyacrylamide Separan AP-273 solutions with concentrations of 300, 500, 700, 1000, 1500 and 2000 w.p.p.m. were used as viscoelestic fluids. Detailed descriptions of other balls, needles and working fluids used in the present study have been offered elsewhere [17].

EXPERIMENTAL RESULTS AND DISCUSSION

Newtonian fluid

Terminal velocities measured in a test cylinder of finite diameter are affected by the ratio of the ball diameter to the cylinder diameter, which is often called 'the wall effect'. Diameter correction formulas for spheres and needles, proposed by Cho [3] and by Park [6], respectively, were used to take into account the cylinder diameter effect and to calculate the terminal velocities in infinite fluids.

The physical properties of the test fluid and falling matter, and the measured terminal velocities, were used to calculate dimensionless parameters such as the Reynolds number and drag coefficients. Figure 2 presents the drag coefficient results for the 92% glycerin solution. Drag coefficients determined by the stainless steel balls and the density-adjusted aluminum balls are in good agreement with the predictions from Stokes law for Reynolds numbers that are less than unity. It is of note that drag coefficients could be determined at very low Reynolds numbers (i.e. 10^{-3}),

Table 3. Dimension and density of needles

Ball No.	Diameter $\times 10^{-3}$ m	Length $\times 10^{-3}$ m	Mass $\times 10^{-3}$ kg	Density (kg m^{-3})	Ratio (L/d)
1	1.56	74.71	0.1910	1346.9	47.89
2	1.55	47.22	0.1343	1523.9	30.46
3	1.56	62.45	0.1572	1328.0	40.03
4	2.34	142.72	1.2320	1979.2	60.99
5	6.21	124.03	4.0112	1059.8	20.45
6	6.21	50.67	1.7629	1197.6	8.15
7	6.22	94.08	4.0572	1451.2	15.12

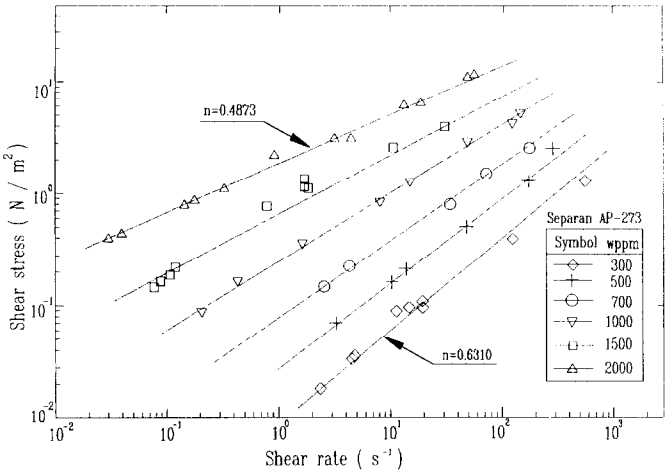

FIG. 3. Shear stress vs shear rate for polyacrylamide Separan AP-273 solutions.

a difficult task for dilute polyacrylamide solutions, by using the density-adjusted aluminum balls in the falling ball viscometer.

Average shear stress and rate of shear

Figure 3 shows experimental values of shear stress, the rate of shear, and the power-law index n of the polyacrylamide solution. In order to calculate the average shear stress and the average rate of shear for a falling ball, the present study used the correction factors C_1 and C_2, which were described in detail by Cho [3]. When a needle was used in the falling ball viscometer, a formula suggested by Park [6] was employed to calculate the average shear stress and the average rate of shear. The power-law index of the 300 w.p.p.m. polyacrylamide solution is 0.6310, whereas the corresponding index of the 2000 w.p.p.m. polyacrylamide solution is 0.4873. The value of the power-law index decreases as the polymer concentration increases.

The characteristic time

In past studies, it was a challenge to measure the viscosity of a low concentration non-Newtonian solution at very low rate of shear in the falling ball viscometer using balls because of the difficulty in measuring the terminal velocity accurately. Hence, the zero-shear-rate viscosity of the non-Newtonian fluid has often been measured by a rotating Couette-type viscometer. The present experiment used density-adjusted aluminum balls in a falling ball viscometer and measured the viscosity of dilute polyacrylamide solutions at the rate of shear as low as 2×10^{-2} (s^{-1}), including the zero-shear-rate viscosity. High shear rate viscosity and the infinite-shear-rate viscosity were determined using a capillary tube viscometer, as mentioned earlier.

Figure 4 presents the apparent viscosities versus shear rate for the polyacrylamide solutions. In the figure, FBV and CTV represent the falling ball viscometer and the capillary tube viscometer, respec-

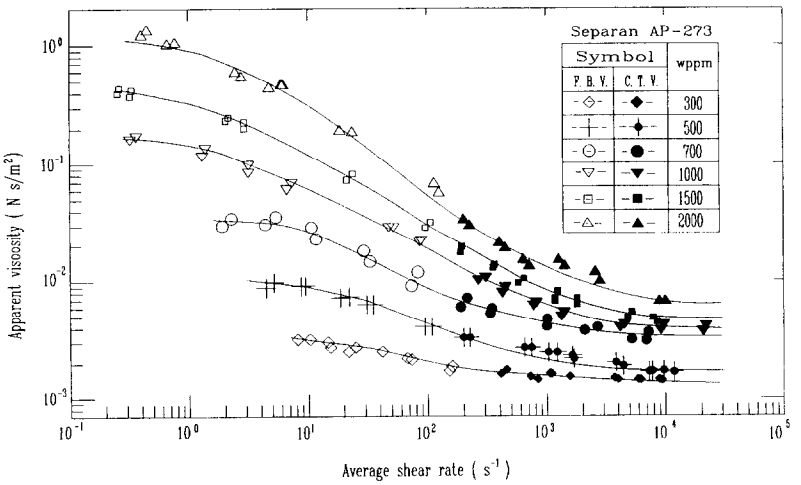

FIG. 4. Apparent viscosity vs average shear rate for polyacrylamide Separan AP-273 solutions. FBV = falling ball viscometer and CTV = capillary tube viscometer.

Table 4. Rheological models for the characteristic time of a polymer solution

Models	Viscosity ($N\ s\ m^{-2}$)	Characteristic time (s)
Powell–Eyring Model [18]	$\eta = \eta_\infty + (\eta_0 - \eta_\infty)\left[\frac{\sinh^{-1}\lambda_1\dot{\gamma}}{\lambda_1\dot{\gamma}}\right]$	λ_1
Chang–Darby [19]	$\eta = \eta_\infty + \frac{(\eta_0 - \eta_\infty)}{(1+\lambda_1^2\dot{\gamma}^2)^{(1-n)/2}}$	λ_1
Cross [20]	$\eta = \eta_\infty + (\eta_0 - \eta_\infty)\frac{1}{1+(\lambda_1\dot{\gamma})^m}$	λ_1
Carreau A [21]	$\eta = \eta_\infty + (\eta_0 - \eta_\infty)[1+(\lambda_1\dot{\gamma})^2]^{(n-1)/2}$	λ_1

tively. As the concentration of the polyacrylamide solutions increases, the difference between the zero-shear-rate viscosity and the infinite-shear-rate viscosity also increases. The apparent viscosity decreases as the rate of shear increases, approaching to an asymptotic value depending on the concentration of the polyacrylamide solution for the rate of shear above 1000 (s^{-1}).

The characteristic time can be calculated by adopting a rheological model (i.e. generalized Newtonian models), as reported in the literature. The present study determined the characteristic times of the polyacrylamide solutions using the apparent viscosity results shown in Fig. 4. Four rheological models were adopted in the present study and the results from each rheological model are given in Table 4.

Figure 5 presents calculated characteristic times, which depend on the concentration of the polyacrylamide solution. Characteristic times increase as the concentration of the polyacrylamide solution increases. The characteristic times calculated by using four models are almost the same, indicating that one can use any one of the rheological models to determine the characteristic time of the polyacrylamide solutions. The Powell–Eyring model among the four models used predicts the largest characteristic time.

The diffusion time

When a ball starts to fall in a fluid the ball is accelerated initially and then approaches its terminal velocity. The terminal velocity of a falling ball in a viscoelastic fluid depends on the time interval between two balls [3, 4]. As the time interval increases, the terminal velocity decreases. As the time interval becomes sufficiently long, the terminal velocity approaches an asymptotic value, which is the value to be obtained when a ball falls in an undisturbed fluid. An increase of the terminal velocity implies a decrease of the apparent viscosity of the non-Newtonian fluid or some change in flow field (i.e. molecular structure or orientation) around the ball. This phenomenon has never been observed in Newtonian or purely viscous non-Newtonian fluids, but in viscoelastic fluids. To illustrate this phenomenon, Cho *et al.* [4] introduced a diffusion time, which is defined as the dropping time interval required to produce 95% of the asymptotic terminal velocity for a given viscoelastic fluid.

Figure 6 presents experimental results for the normalized viscosity and dropping time interval in the falling ball viscometer. The normalized viscosity is the ratio of the viscosity at a certain time interval to the viscosity of the asymptotic value. Since the normalized viscosity approaches the asymptotic value almost exponentially, the value of the diffusion time can be significantly different depending on whether 95 or

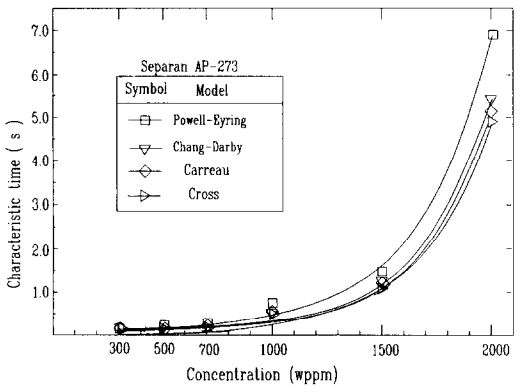

FIG. 5. Characteristic times for polyacrylamide Separan AP-273 solutions. Powell–Eyring [18], Chang–Darby [19], Carreau [21] and Cross [20].

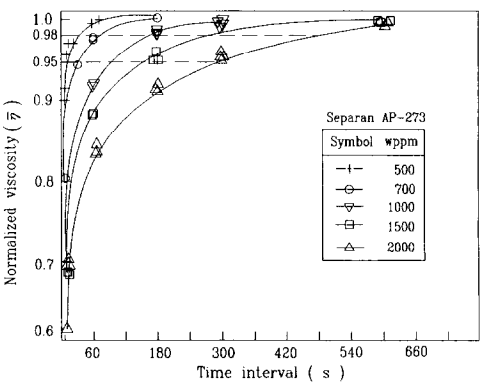

FIG. 6. Normalized viscosity vs time interval for polyacrylamide Separan AP-273 solutions.

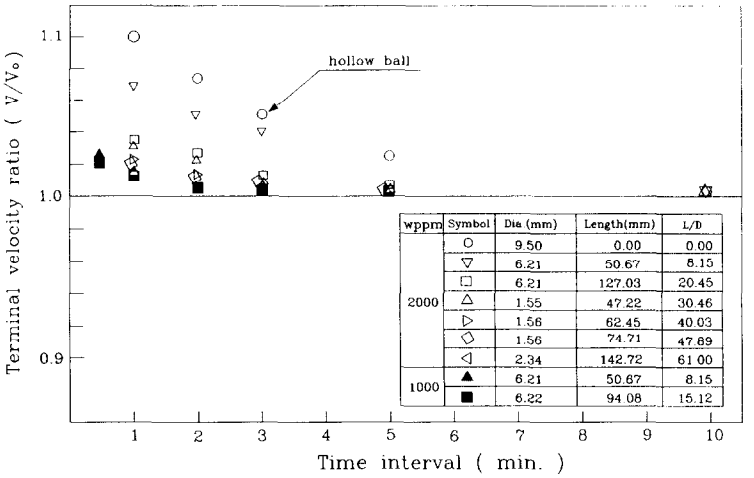

FIG. 7. Terminal velocity vs time interval for polyacrylamide Separan AP-273 solutions. Open circles represent data obtained with hollow aluminum balls, and all other symbols with needles.

98% of the asymptotic value is used in the determination of the diffusion time. Considering that the diffusion time occurs as a flow phenomenon and that the diffusion time is determined by experimental result, the present study adopts the 98% criterion.

Figure 7 presents normalized terminal velocities with density-adjusted aluminum balls (i.e. open circles) and needles (i.e. all other symbols) with different ratios of length to diameter in the aqueous polyacrylamide solutions. For a given fluid and a given time interval, the terminal velocities depend on the types of balls and needles used. In particular, the terminal velocities of needles are strongly dependent on the ratio of length to diameter. For a fixed time interval, the terminal velocity of a needle decreases as the ratio of length to diameter increases. The terminal velocity of the needle becomes almost independent of the ratio when the ratio exceeds 48 in the 2000 w.p.p.m. solution. This observation for the terminal velocity of needles with large length-to-diameter ratios is in good agreement with the experimental study of Park and Irvine [7], who reported that the diffusion time was not detected when the needles were sufficiently long. Therefore, if one wants to measure the viscosity of a viscoelastic fluid with a needle, one with a length-to-diameter ratio greater than 48 should be used, thus eliminating the effect of diffusion time on the viscosity measurement.

Degradation effects

Aqueous polyacrylamide solutions were recirculated in a flow loop with a positive displacement pump to investigate the rheological property changes of the solutions due to mechanical degradation. The diameter of the test tube was $D = 1.03$ cm and the length-to-diameter ratio was $x/D = 1160$. The Reynolds number was varied in the range of 20 000–45 000. Fluid samples were taken out of the flow loop at regular time intervals, and viscosities of the samples were measured both in the falling ball viscometer and in the capillary tube viscometer. For the polyacrylamide solution tested in the present study, the characteristic time was calculated from the Powell–Eyring model, and the diffusion time was determined by the aforementioned 98% criterion.

Figure 8 presents the changes in the characteristic time due to degradation for the 300, 700 and 1000 w.p.p.m. polyacrylamide solutions. The characteristic time changes rapidly during the initial period of degradation and levels off as degradation continues. After 12 h of recirculation the characteristic time reaches an asymptotic value for each polyacrylamide solution. This observation is consistent with the observations reported by Cho and Hartnett [22].

Figure 9 presents the apparent viscosity changes of the 1000 w.p.p.m. polyacrylamide solution due to degradation. Viscosities at low shear rates (i.e. 0.3 s^{-1}) were measured with density-adjusted balls in the falling ball viscometer, whereas those at high shear rates were measured using the capillary tube viscometer. At the initial stage of degradation, the

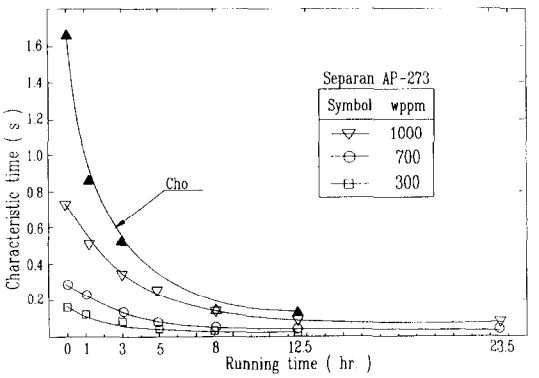

FIG. 8. Characteristic time vs running time for polyacrylamide Separan AP-273 solutions.

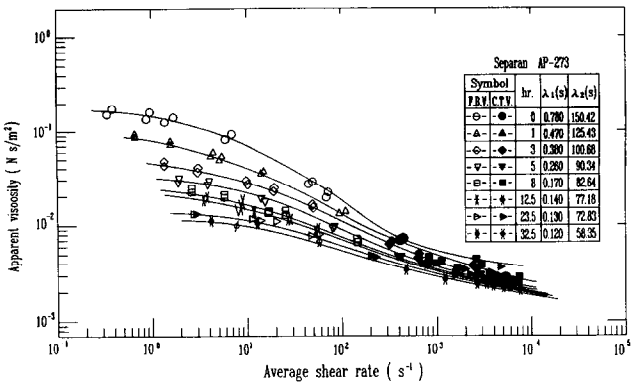

FIG. 9. Degradation effect on the apparent viscosity for 1000 w.p.p.m. polyacrylamide Separan AP-273 solutions. λ_1 = characteristic time calculated from Powell–Eyring model and λ_2 = diffusion time.

decrease of the zero-shear-rate viscosity is quite pronounced, but that of the infinite-shear-rate viscosity is not.

The degrading polyacrylamide solution exhibits quite different characteristic time and diffusion time from those of the fresh solution, depending on the degree of degradation. As degradation continues, both the characteristic time (λ_1) and the diffusion time (λ_2) decrease. For the case of the 1000 w.p.p.m. polyacrylamide solution, the characteristic time decreased from 0.78 to 0.12 s after 12.5 h recirculation whereas the diffusion time decreased from 150.42 to 58.35 s. The comparison between the two times indicates that the diffusion time was less sensitive to degradation than the characteristic time.

Figure 10 presents the results of both the friction factor and heat transfer coefficients for the polyacrylamide solution undergoing mechanical degradation. The heat transfer coefficient increases much more rapidly from the minimum heat transfer asymptote introduced by Eum [16] in the beginning of degradation than the friction coefficient does. On the whole, the degradation effect on the heat transfer is more serious than on the friction factor during the initial period of degradation.

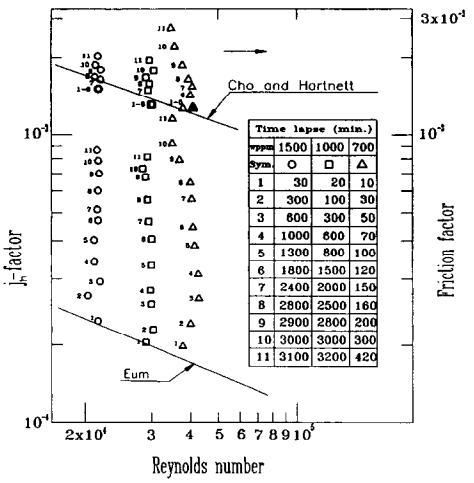

FIG. 10. Degradation effect on friction factor and heat transfer coefficient for polyacrylamide Separan AP-273 solutions. Cho and Hartnett [22] represents the minimum friction asymptote, and Eum [16] represents the minimum heat transfer asymptote which is given as $j_h = 0.093(x/D)^{-0.34} Re_a^{-0.36}$.

Flow visualization

The primary purpose of the visualization was to relate the diffusion time of a viscoelastic fluid observed in a falling ball viscometer to the flow field change around the ball. In order to visualize the flow structure around falling balls, a particle method which uses a light sheet and a digital image-processing technique [23] was applied. Since the present study focused on the flow around balls dropped at certain time intervals traveling along the centerline of the test container, a special technique in the application of fluorescent dye was employed.

Butyl aniline powder, which is made up of fluorescent dye-coated micron-size particles, was stained on the front portion of balls. Since the balls were dropped along the centerline of the test container, the butyl aniline powder made approximately 2 mm thick lines along the centerline. When an actual flow image was taken, a ball without the butyl aniline powder was dropped. The thick lines produced by previous balls along the center of the container manifested the effect of the falling ball on the local flow structure upstream and downstream of the ball. This technique gave much clearer streamline results than the technique using evenly dispersed particles could have given. Using a light sheet and a digital image processing technique [23], the flow structure was captured by a CCD (charge-coupled device) camera and stored in an IBM PC computer. The flow image was further processed by a digital image enhancement software called PC Vision Plus.

Figure 11 shows the flow visualization results of the flow field around a sphere for two different time intervals. When the time interval is 3 min, recirculating eddies are shown both upstream and downstream of the falling ball. As the time interval increases

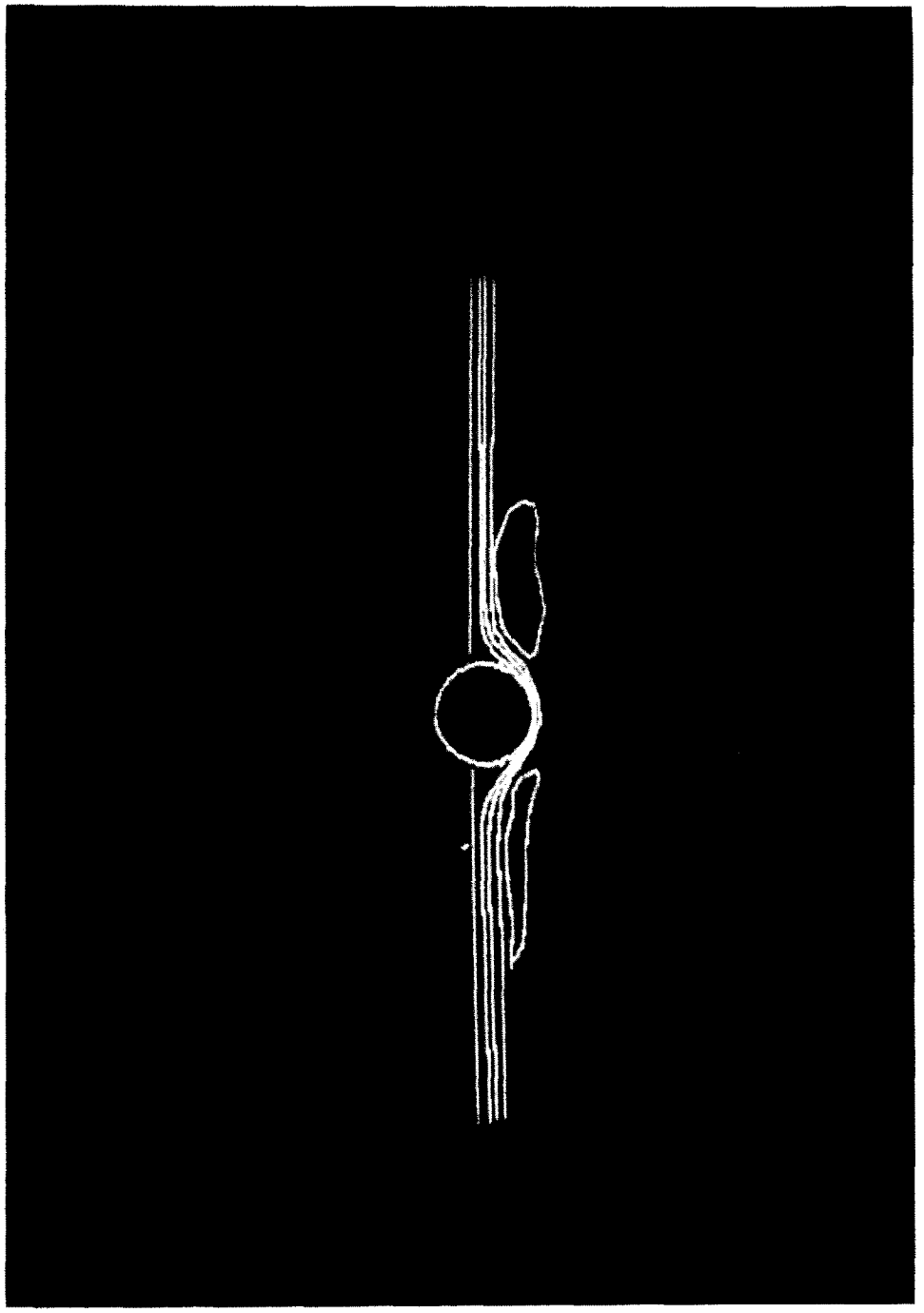

(a)

FIG. 11. Streamline pattern around a sphere for 2000 w.p.p.m. polyacrylamide Separan AP-273 solutions. (a) Time interval = 3 min, (b) time interval = 10 min.

to 10 min, the eddies disappear and the flow patterns in the front and back of the falling ball are asymmetric to each other. The flow visualization test was repeated for Newtonian fluids (i.e. diluted glycerin solutions); the above-mentioned phenomena have not been observed in the Newtonian fluids at the low Reynolds numbers used in the present study.

SUMMARY

The present study attempted to measure the rheological properties of drag-reducing polyacrylamide solutions (both fresh and those undergoing mechanical degradation). Falling balls and needles were used to yield steady shear viscosities of the poly-

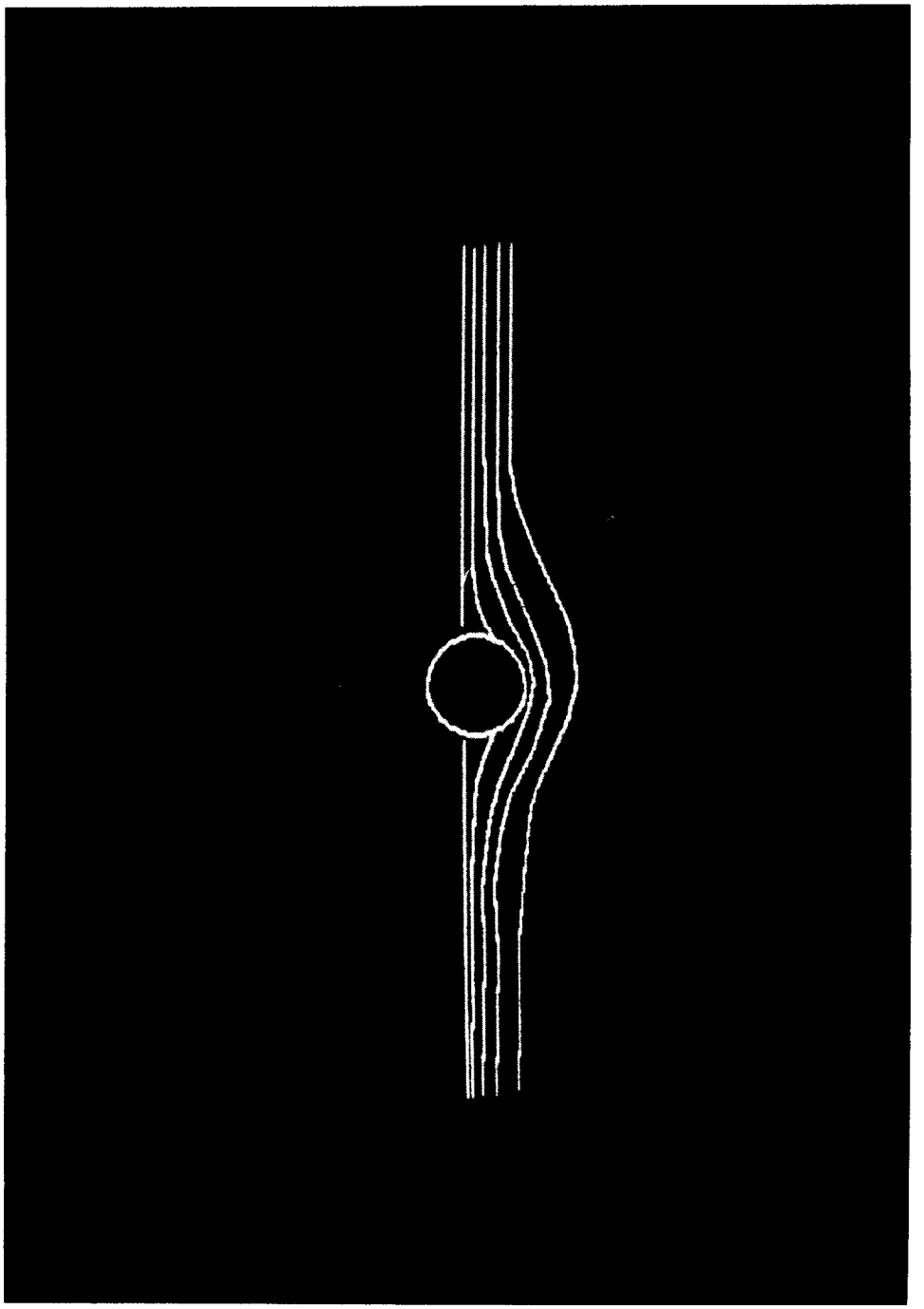

(b)

FIG. 11—*Continued.*

acrylamide solutions over a wide range of shear rate in order to determine the characteristic time and diffusion time of the solutions. The following points summarize the key findings.

(1) A characteristic time was observed even for a low concentration polyacrylamide solution. The characteristic time increased as the polyacrylamide concentration increased. The Powell–Eyring model predicted the largest characteristic time among four rheological models tested.

(2) The diffusion time of the polyacrylamide solution was observed when a ball was used in the falling ball viscometer. The diffusion time increased as the polyacrylamide concentration increased.

(3) The diffusion time was also observed with a falling needle if its length-to-diameter ratio was less than 48. As the ratio of length to diameter of the

needle increased beyond 48, the diffusion time of the polyacrylamide solution reduced to almost zero.

(4) As the polyacrylamide solution degraded, the zero-shear-rate viscosity decreased more rapidly than the infinite-shear-rate viscosity. Both the characteristic time and the diffusion time decreased as the polyacrylamide solution degraded.

(5) The effect of degradation on heat transfer was more serious than that on the friction factor during the initial period of degradation.

Acknowledgement—The first author would like to express his appreciation to the Advanced Fluids Engineering Research Center, financed by the Korea Science and Engineering Foundation, for financial assistance.

REFERENCES

1. R. M. Turian, An experimental investigation of the flow of aqueous non-Newtonian high polymer solutions past a sphere, *A.I.Ch.E. Jl* **13,** 999–1006 (1976).
2. M. Gottlieb, Zero shear rate viscosity measurements for polymer solutions by falling ball viscometer, *J. Non-Newtonian Fluid Mech.* **6,** 97–109 (1979).
3. Y. I. Cho, The study of non-Newtonian flows in the falling ball viscometer, Ph.D. Thesis, University of Illinois at Chicago (1979).
4. Y. I. Cho, J. P. Hartnett and W. Y. Lee, Non-Newtonian viscosity measurements in the intermediate shear rate range with the falling ball viscometer, *J. Non-Newtonian Fluid Mech.* **15,** 61–74 (1984).
5. D. Kanchanalakshana and A. J. Ghajar, An improved falling sphere viscometer for intermediate concentrations of viscoelastic fluids, *Int. Commun. Heat Mass Transfer* **13,** 219–233 (1966).
6. N. A. Park, Measurement of rheological properties of non-Newtonian fluids with falling needle viscometer, Ph.D. Thesis, State University of New York at Stony Brook (1984).
7. N. A. Park and T. F. Irvine, Jr., The falling needle viscometer—a new technique for viscosity measurements, *Wärme- und Stoffübertragung* **18,** 201–206 (1984).
8. D. F. James and A. J. Acosta, The laminar flow of dilute polymer solutions around circular cylinder, *J. Fluid Mech.* **42,** 269–288 (1970).
9. A. B. Metzner, Behavior of suspended matter in rapidly accelerating viscoelastic fluids: the Uebler effect, *A.I.Ch.E. Jl* **13,** 316–318 (1967).
10. A. B. Metzner and J. L. White, Flow behavior of viscoelastic fluids in the inlet region of a channel, *A.I.Ch.E. Jl* **11,** 989–994 (1965).
11. A. B. Metzner, E. A. Uebler and C. F. Fong, Converging flow of viscoelastic materials, *A.I.Ch.E. Jl* **15,** 750–758 (1969).
12. W. J. Yang, *Flow Visualization III.* Hemisphere, New York (1985).
13. W. J. Yang and Y. Chen, Advances and perspectives in flow visualization. In *Fluids Engineering Seminar Korean–U.S. Progress*, pp. 349–368 (1986).
14. S. M. Choi, J. W. Kim and J. M. Hyun, Transient free surface shape in an abruptly rotating partially filled cylinder, *J. Fluids Engng* **111,** 439–442 (1989).
15. T. S. Whang, A study on the heat transfer of viscoelastic non-Newtonian fluids in turbulent channel flows, Ph.D. Thesis, Dankook University, Seoul, Korea (1988).
16. J. S. Eum, A study on the heat transfer augmentation of the viscoelastic fluids in circular tube flows, Ph.D. Thesis, Dankook University, Seoul, Korea (1988).
17. C. Y. Jeon, A study on the characteristic time and viscosity of viscoelastic fluids using the ball and needle, Ph.D. Thesis, Dankook University, Seoul, Korea (1988).
18. R. E. Powell and H. Eyring, Mechanisms for the relaxation theory of viscosity, *Nature* **154,** 427 (1944).
19. H. D. Chang and R. Darby, Generalized correlation for friction loss in drag reducing polymer solutions, *A.I.Ch.E. Jl* **30,** 274–280 (1984).
20. M. M. Cross, Rheology on non-Newtonian fluids: a new flow equation for pseudo plastic systems, *J. Colloid Sci.* **20,** 417–437 (1965).
21. P. J. Carreau, Rheological equations from molecular network theories, *Trans. Soc. Rheol.* **16,** 99 (1972).
22. Y. I. Cho and J. P. Hartnett, *Non-Newtonian Fluids, Handbook of Heat Transfer Applications*, Chap. 2, pp. 1–50. McGraw-Hill, New York (1986).
23. C. R. Smith, *Computer-aided Flow Visualization, Handbook of Flow Visualization* (Edited by W. J. Yang), Chap. 24, pp. 375–391. Hemisphere, New York (1989).